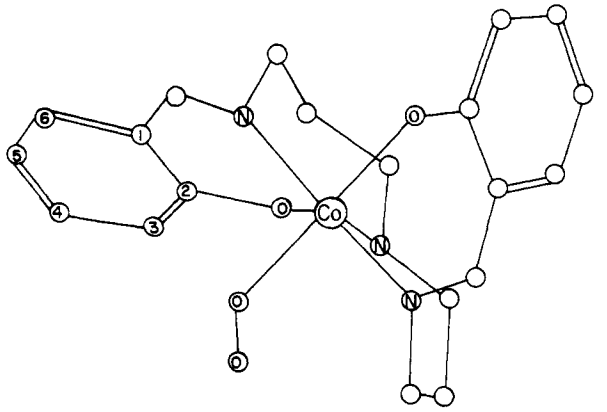

Figure 3. Proposed configuration of the cobalt dioxygen catalyst, CoSMDPT, based on the μ-peroxy dimer.[16a]

Figure 3) or a geometric rearrangement[16a,b] of the complex increases the binding of O_2 to the cobalt over that expected from the electron withdrawing substituent effect. Electron transfer and kinetic results from ligands with a *tert*-butyl group in the three positions suggest that the polar effect may be more significant.

The catalyst half-life ($\tau_{1/2}$) is obtained when the reaction rate has dropped to one-half of the initial rate. The number of turnovers recorded at the catalyst half-life ($\tau_{1/2}$) will be one-half of the total number of turnovers expected if the decomposition pathway is first order in catalyst concentration. In most instances the number of turnovers recorded after 24 h (several half-lives) is significantly greater than expected for a first-order process. This indicates that decomposition due to dimerization of the cobalt complexes or hydrogen atom abstraction of the ligand by a proximal cobalt dioxygen complex could be contributing to catalyst degradation. Also, it has been shown that the product quinone can prevent decomposition of the catalyst presumably by serving as a trap for reactive species that may degrade the catalyst.[7] The fact that high loading of the substrate phenol leads to an elevated number of turnovers and longer half-life suggests that the substrate itself is capable of protecting the catalyst, either by trapping small amounts of reactive products or by hydrogen bonding to the catalyst and blocking access to the cobalt complex. Finally, the catalyst stability does not manifest a meaningful trend in the SMDPT series. There is significant enhancement of stability for the 5-Br derivative.

The large number of turnovers attained with both the 4,6-dimethoxy and the 3,5-dibromo derivatives indicate that ring substitution stabilizes the catalyst. Attack of the ring by H_2O_2 can lead to ring cleavage and conversion to carboxylic acids. Thus, substituents leading to increased turnovers may block ring attack. The production of significant quantities of the coupled quinone with the *tert*-butyl-substituted CoSMDPT catalyst also suggests that the rate-determining step of the cobalt dioxygen attack on the phenoxy radical is becoming sterically restricted for these bulky substituents in the three position. The steric bulk of the *tert*-butyl groups is not great enough to prevent the initiation step involving the formation of the 2,6-di-*tert*-butyl phenoxy radical or its subsequent generation through the reduction of the cobalt catalyst (Figure 1, step d).

Acknowledgment. The authors acknowledge, with thanks, the support of this research by the National Science Foundation through Grant CHE 82 13398. R.P.P. appreciates the support provided by a DuPont fellowship.

(16) (a) Lindblom, L. A.; Schaefer, W. P.; Marsch, R. E. *Acta Crystallogr., Sect. B* **1971**, *27B*, 1461. (b) Cini, R.; Orioli, P. *J. Chem. Soc., Dalton Trans.* **1983**, 2563. X-ray single-crystal studies on crystals of the μ-peroxy-dimer [{CoSMDPT}$_2$O$_2$] grown from either toluene[16a] or benzene[16b] solvent have resulted in two different isomers. Figure 2 represents the isomers found in ref 16b where the immine and phenolic donors are in the equatorial plane and the amine trans to the bound O_2, and Figure 3 represents the structure found in ref 16a. Clearly, both isomers may be present in solution, the relative amount determined by the solvent dielectric and the ring substituents.

Mechanistic Considerations in the Photodisproportionation of μ-Oxo-bis((tetraphenylporphinato)iron(III))

Mark W. Peterson, David S. Rivers, and Robert M. Richman*

Contribution from the Department of Chemistry, Carnegie-Mellon University, Pittsburgh, Pennsylvania 15213. *Received September 20, 1984*

Abstract: The photochemistry of μ-oxo-bis((tetraphenylporphinato)iron(III)) [(FeTPP)$_2$O] has been studied. Both continuous and flash photolysis establish a photochemical disproportionation to form the ferrous complex FeTPP and the ferryl complex FeOTTP. Using triphenylphosphine to trap the ferryl complex results in a net formation of FeTTP. This reaction is found to be intensity dependent at sufficiently high lamp intensities ($I_0 > 10^{-8}$ einstein), and these data have been computer fitted to the photodisproportionation mechanism. Olefins (cyclohexene and tetramethylethene) were found to react with the ferryl complex at high intensities to yield the ene-ol. Catalytic oxidation of cyclohexene was performed in the presence of dioxygen in sunlight to yield 2-cyclohexen-1-one with >1000 turnovers of the (FeTPP)$_2$O. There is no temperature dependence. The quantum yield increases with decreasing wavelength in the range λ 350–440 nm. This favors photochemistry from a highly distorted metal-to-metal charge-transfer state.

Several common elements emerge from a study of the most promising strategies for solar energy conversion. From semiconductor electrodes to photosynthesis, photon energy is initially converted to charge separation. Efficient mechanisms prevent immediate loss of this energy as heat in a back reaction. Whether by band bending[1] or subsequent electron transfer steps,[2] a small amount of stored energy is sacrificed to further separate the charge pair. This charge can then do useful oxidation–reduction reactions. In solutions of synthetic compounds, epitomized by $Ru(bpy)_3^{2+}$, exploitation utilizes these same elements.[3] Photon energy is used to generate a charge-transfer excited state, and further separation of charge is achieved by bimolecular quenching which is fast with respect to back reaction. The oxidized and reduced species so generated are then capable of doing useful redox work. The search

(1) Wrighton, M. S.; Kaiser, S. W. *Adv. Chem. Serv.* **1977**, *163*, 71.
(2) Bolton, J. R. "Solar Energy: Chemical Conversion and Storage;" R. R. Hautala, R. B. King, and C. Kutal, Ed.; Humana, 1979, p 31.
(3) Sutin, N. *J. Photochem.* **1979**, *10*, 19.

0002-7863/85/1507-2907$01.50/0

for synthetic systems of promise has thus been limited to compounds with long-lived charge-transfer excited states. Transition-metal complexes have drawn the most interest, because they usually absorb in the solar spectrum and have several stable oxidation states. But most transition-metal complexes have excited states that are dissociative, and many are too short-lived to undergo bimolecular quenching.[4] We have sought to elucidate an alternative strategy for solar energy conversion using transition-metal complexes that are dissociative and do not necessarily have long-lived excited states.

Gray and co-workers have generated hydrogen photochemically from aqueous acid containing the complex of rhodium(I) and 1,3-diisocyanopropane (abbreviated $Rh_2(bridge)_4^{2+}$, or in the following D for dimer). Flash studies established the following mechanism.[5]

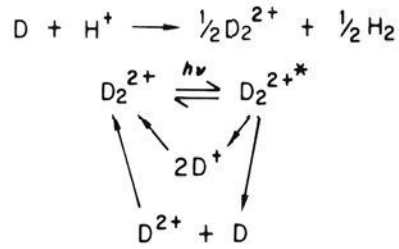

The photoactive blue compound is apparently a dimer of dimers. The excited state can deactivate by either homolytic or heterolytic cleavage of a rhodium–rhodium bond. The former results in recombination to the ground-state molecule, but the latter gives D, a reducing agent strong enough to produce hydrogen. Energy storage is obtained from a short-lived, non-luminescent excited state undergoing rapid dissociation. The key is this mode of dissociation, a mode we term *photodisproportionation*. One product is a stronger oxidant than the reactant and may do a useful oxidation at a rate competitive with back reaction. The other product is a stronger reductant than the reactant and may do a useful reduction at a rate competitive with back reaction. Photochemical energy can be stored if *either* of these conditions is met.

Another class of compounds subject to photodisproportionation is oxo-bridged dimers. Here, because of the way electrons are counted in an oxidation state formalism, it is *homolytic* cleavage that leads to disproportionation

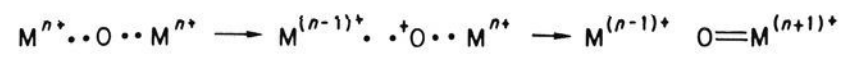

Once again, the products may include a useful reductant or a useful oxidant. But there is the additional possibility that M=O is capable of doing useful, selective atom transfers, as the following example illustrates:

$$M{-}O{-}M \xrightarrow{h\nu} M{=}O + M$$
$$M{=}O + R \rightarrow M + RO$$
$$2M + {}^1/_2O_2 \rightarrow M{-}O{-}M$$

Photodisproportionation should be a commonly encountered mode of photodissociation because the valence bond treatment of the singlet-coupled $\sigma \rightarrow \sigma^*$ state[6] may be generalized to encompass, for example, a transition of the type shown in Figure 1 for an M—O—M complex. The $\pi_n \rightarrow \pi^*$ transition is a fully allowed d–d transition. The singlet-coupled excited state is

$$(1/\sqrt{2})d_{yz}^{(1)}(1)d_{yz}^{(1)}(2) - d_{yz}^{(2)}(1)d_{yz}^{(2)}(2)$$

This state can also be written as

$$(1/\sqrt{2})[(M^-OM^+) - (M^+OM^-)]$$

the valence bond ionic configuration.

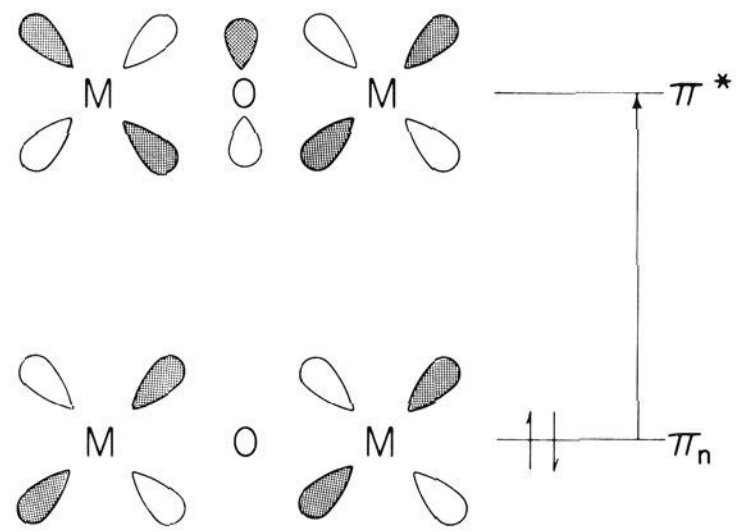

Figure 1. Molecular orbital transition equivalent to a valence bond metal-to-metal charge transfer.

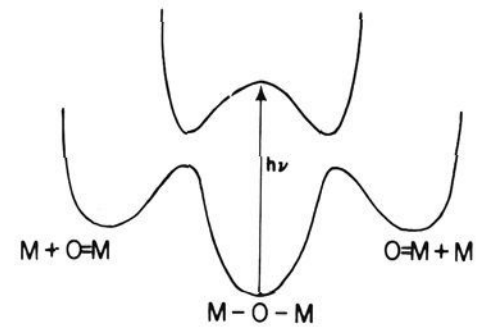

Figure 2. Potential energy diagram for photochemical disproportionation. The x axis represents the antisymmetric M–O–M vibration.

This excited state is essentially a metal-to-metal charge-transfer state. It should be prone to disproportionation. Indeed, this transition is formally equivalent to the $\Delta Z = 2$ intervalence transfer transition discussed by Allen and Hush.[7]

Regardless of the precise electronic nature of the excited state, the potential energy diagram for the thermal and photochemical processes must surely resemble Figure 2. Here the X coordinate is primarily the M–O–M antisymmetric vibration. Net photochemistry occurs in the nonadiabatic process of crossing from the upper surface to the lower one. Only some fraction of the photochemical energy is stored in the products. The remaining "lost" energy is concentrated in that degree of freedom which thrusts the products in opposite directions, most effectively separating the reactive fragments. Thus photodisproportionation shares with other promising strategies a propensity to sacrifice some of its stored energy in order to minimize back reaction.

Many transition metals represent strong oxidants in various enzymes. Perhaps the most widely studied of the metals is iron.[8–11] Iron porphyrins fulfill roles in electron-transfer proteins, oxygen-transfer proteins, and catalysts for oxygen insertion into biological substrates.

Of particular interest here are the roles of iron porphyrins in both oxygen transfer and electron transfer. Two such enzymes that have attracted much interest are cytochrome P-450 (P450) and horseradish peroxidase (HRP). Both of these enzymes catalyze the oxidation of biological substrates and have a resting iron site that contains ferriprotoporphyrin IX.[10] The mechanisms and oxidation states of the active sites have been widely studied.

Many workers have studied synthetic metalloporphyrins in an attempt to mimic the behavior of these enzymes.[12–29] Of particular

(4) Adamson, A.; Fleischauer, P. "Concepts of Inorganic Photochemistry"; Wiley: New York, 1975.
(5) Sigal, I. S.; Mann, K. R.; Gray, H. B. *J. Am. Chem. Soc.* **1980**, *102*, 7252.
(6) Lecture Notes from W. A. Goddard, California Institute of Technology, 1976.
(7) Allen, G. C.; Hush, N. S. *Prog. Inorg. Chem.* **1967**, *8*, 357.
(8) Smith, K. M. "Porphyrins and Metalloporphyrins"; Elsevier: New York, 1975.
(9) Dolphin, D. "The Porphyrins"; Academic Press: New York, 1978.
(10) Gray, H. B.; Lever, A. B. P. "Iron Porphyrins"; Addison-Wesley: Reading, MA, 1983.
(11) Sheldon, R. A.; Kochi, J. K. "Metal-Catalyzed Oxidations of Organic Compounds"; Academic Press: New York, 1981.
(12) Groves, J. T.; Nemo, T. E.; Myers, R. S. *J. Am. Chem. Soc.* **1979**, *101*, 1032.
(13) Groves, J. T.; Kruper, W. J.; Nemo, T. E.; Myers, R. S. *J. Mol. Catal.* **1980**, *7*, 169.

interest is the work of Groves and co-workers.[27-30]

They have demonstrated the ability of (chloro)iron(III) porphyrins (FeTPPCl and FeTMPCl, TPP = tetraphenylporphyrin and TMP = tetramesitylporphyrin) to mediate the iodosobenzene oxidation of olefins and alkanes.[28,29] The systems studied convert unactivated, saturated C–H bonds to the corresponding alcohols, and olefins are stereoselectively epoxidized. The active complex is believed to be a ferryl porphyrin radical cation, and an electron-transfer mechanism is favored.

While many attempts have been made at obtaining synthetic iron(IV) porphyrin complexes, few have succeeded in forming a true iron(IV) oxidation state; rather, most have resulted in the formation of iron(III) porphyrin radical cations.[31-34] The only reliable report of a true ferryl complex has been by Balch and La Mar for TPP ($Fe^{IV}OTPP$).[35,36] Their studies of the oxidation of FeTPP by O_2 result in a stable iron(III) peroxo-bridged complex at −80 °C. If, however, the temperature is raised above −30 °C or an appropriate base is added (pyridine, piperidine, or imidazole), the ferryl complex formed is FeOTPP or BFeOTPP, respectively. Balch has also demonstrated a quasicatalytic oxidation of triphenylphosphine at −80 °C as follows:

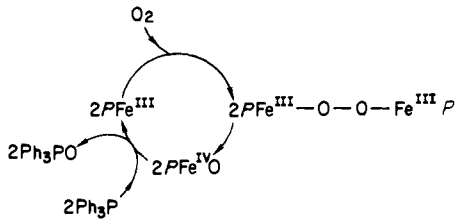

While these results are quite interesting, the true oxidative nature of the ferryl complex at ambient temperatures is still in question. The properties of an uncoordinated "ferryl" complex ($Fe^{IV}OTMP$) are only now being addressed,[37] and with great difficulty since this complex abstracts hydrogen atoms from solvent above −30 °C.

These results support the hypothesis that the ferryl complex of TPP ($Fe^{IV}OTPP$) that would be expected from the photodisproportionation of the known dimer $(FeTPP)_2O$[38] should be at least a strong one-electron oxidant (like HRP-II) and may have the potential for two-electron oxidations by a radical mechanism similar to that proposed by Groves for the hydroxylation of olefins. Photodisproportionation of $(FeTPP)_2O$ would also allow for the generation of FeOTPP or BFeOTPP at ambient temperatures and the study of their oxidative properties.

$(FeTPP)_2O$ generally does not coordinate axial ligands (i.e., $(L\text{–}FeTPP)_2O$) and has only one tetradentate ligand per metal. As a result, one would not expect ligand dissociation (either homolytic or heterolytic). $(FeTPP)_2O$ is thermally inert and shows no monomer/dimer equilibrium.[39] It can be oxidized by both one and two electrons[32-34] or reduced by one electron[40] and maintain the μ-oxo structure. Furthermore, the ferrous complex (FeTPP) that would be expected from disproportionation is thermally inert in the absence of oxygen and has been well characterized in many solvents with various axial ligands.[41,42]

There have been several photochemical studies of iron(III) porphyrins that have demonstrated their ability to do redox photochemistry. Among these studies are photostudies of alcohol-coordinated complexes.

Bartocci et al.[43] and Brault et al.[44] have demonstrated the ability of the nonemitting porphyrin complexes iron(III) protoprophyrin IX chloride and iron(III) deuteroporphyrin chloride to do redox photochemistry in the presence of alcohols. In each case, the actual complex is an alcoxy complex (not the chloride) and the primary photostep is homolytic cleavage of the iron–oxygen bond as demonstrated by both flash photolysis and identification of the alcohol radical products. Both authors consider the photochemistry due to ligand-to-metal charge transfer, but neither speculates as to where such a transition exists.

Recently we communicated the initial evidence for the photodisproportionation of $(FeTPP)_2O$.[45] Here we present a more complete experimental and theoretical treatment of this prototype for solar energy conversion schemes.

Experimental Section

Compounds and Materials. $(FeTPP)_2O$ was obtained from Strem Chemical Co. The complex was found to contain trace H_2TPP impurities by fluorescence spectroscopy. This was removed by recrystallization and chromatography on neutral alumina.

Triphenylphosphine (PPh_3), phenyl-*tert*-butylnitrone (PBN), spectral quality tetramethylethene, benzene, and 1,2-dichloroethane were obtained from Aldrich Chemical Co. and used without further purification. Spectral grade pyridine obtained from Aldrich was periodically distilled. Piperidine (97%) obtained from Aldrich was distilled over KOH. Cyclohexene 99% obtained from Aldrich was distilled once and then again prior to use.

Quantum Yield Determination. The quantum yields were determined as we have described.[55] FeTPP represents the ultimate photoproduct and is extremely O_2 sensitive, so all samples were freeze–pump–thaw degassed through a minimum of three cycles.

Flash Photolysis. We have previously described the apparatus used to obtain transient spectra.[55] To eliminate the possible misinterpretation of the observed transient spectra due to instrument artifacts, solvent impurities, or free porphyrin, blank runs were made of solvent and solvent plus H_2TPP. No transients were observed when pure solvent was run; however, free H_2TPP gave a nice spectrum. Substantial bleaching is observed at 425 nm and a growth at 452 nm. No similarities were observed between the free H_2TPP transient spectrum and the metalloporphyrin transient spectra reported here.

(14) Change, C. K.; Kuo, M.-S. *J. Am. Chem. Soc.* **1979**, *101*, 3413.
(15) Mansuy, D.; Bartoli, J.-F.; Chottard, J.-C.; Lange, M. *Angew. Chem., Int. Ed. Engl.* **1980**, *19*, 909.
(16) Shannon, P.; Bruice, T. C. *J. Am. Chem. Soc.* **1981**, *103*, 4580.
(17) Hill, C. L.; Schardt, B. C. *J. Am. Chem. Soc.* **1980**, *102*, 6374.
(18) Groves, J. T.; Kruper, W. J., Jr.; Haushalter, R. C. *J. Am. Chem. Soc.* **1980**, *102*, 6375.
(19) Hill, C. L.; Smegal, J. A. *Nov. J. Chim.* **1982**, *6*, 287.
(20) Tabushi, I.; Koga, N. *Tetrahedron Lett.* **1979**, 3681.
(21) Tabushi, I.; Koga, N. *Tetrahedron Lett.* **1978**, 5017.
(22) Tabushi, I.; Yazaki, A. *J. Am. Chem. Soc.* **1981**, *103*, 7371.
(23) Tabushi, I.; Koga, N. *J. Am. Chem. Soc.* **1979**, *101*, 6456.
(24) Peree-Fauvet, M.; Gaudemer, A. *J. Chem. Soc., Chem. Commun.* **1981**, 874.
(25) Groves, J. T.; Kruper, W. J., Jr. *J. Am. Chem. Soc.* **1979**, *101*, 7613.
(26) Groves, J. T.; Takahashi, T. *J. Am. Chem. Soc.* **1983**, *105*, 2073.
(27) Groves, J. T.; Haushalter, R. C.; Nakamura, M.; Nemo, T. E.; Evans, B. J. *J. Am. Chem. Soc.* **1981**, *103*, 2884.
(28) Groves, J. T.; Nemo, T. E. *J. Am. Chem. Soc.* **1983**, *105*, 6243.
(29) Groves, J. T.; Nemo, T. E. *J. Am. Chem. Soc.* **1983**, *105*, 5786.
(30) Groves, J. T.; McClusky, O. A.; White, R. E.; Coon, M. J. *Biochem. Biophys. Res. Commun.* **1978**, *81*, 154.
(31) Felton, R. H.; Owen, G. S.; Dolphin, D.; Forman, A.; Borg, D. C.; Fajer, J. *Ann. N. Y. Acad. Sci.* **1973**, *206*, 504.
(32) Goff, H. M.; Phillippi, M. A. *J. Am. Chem. Soc.* **1982**, *104*, 6026.
(33) Shimomara, E. T.; Phillippi, M. A.; Goff, H. M.; Schola, W. F.; Reed, C. A. *J. Am. Chem. Soc.* **1981**, *103*, 6778.
(34) Phillippi, M. A.; Goff, H. M. *J. Am. Chem. Soc.* **1979**, *101*, 7641.
(35) Chin, D.-H.; Balch, A. L.; La Mar, G. N. *J. Am. Chem. Soc.* **1980**, *102*, 1446.
(36) Chin, D.-H.; La Mar, G. N.; Balch, A. L. *J. Am. Chem. Soc.* **1980**, *102*, 5945.
(37) Balch, A. L., private communication.
(38) Fleischer, E. B.; Srivastava, T. S. *J. Am. Chem. Soc.* **1969**, *91*, 2403.
(39) Fleischer, E. B.; Palmer, J. M.; Srivastava, T. S.; Chatterjee, A. *J. Am. Chem. Soc.* **1971**, *93*, 3162.
(40) Kadish, K. M.; Larson, G.; Lexa, D.; Momenteau, M. *J. Am. Chem. Soc.* **1975**, *97*, 282.
(41) Brault, D.; Rougee, M. *Biochemistry* **1974**, *13*, 4591.
(42) Kobayashi, H.; Yanagawa, Y. *Bull. Chem. Soc. Jpn.* **1972**, *45*, 450.
(43) Bartocci, C.; Scandola, F.; Ferri, A.; Carassiti, V. *J. Am. Chem. Soc.* **1980**, *102*, 7067.
(44) Bizet, C.; Morliere, P.; Brault, D.; Delgado, O.; Bazin, M.; Suntus, R. *Photochem. Photobiol.* **1981**, *34*, 315.
(45) Richman, R. M.; Peterson, M. W. *J. Am. Chem. Soc.* **1982**, *104*, 5795.

Samples were prepared in 1,2-dichloroethane under argon and then placed in either a 0.1 or 0.2 cm quartz cell and purged with argon. All samples were mixed after excitation and replaced after about ten runs to prevent any permanent products from building up in local areas.

Kinetic Fits. In order to simulate the variation in concentration of $(FeTPP)_2O$ and PPh_3FeTPP as a function of time, a computer program was written based on the Bulirsch–Stoer algorithm.[46] This determines approximate solutions to a system of first-order differential equations, given initial values. This algorithm was chosen over the conventional Runge–Kutta algorithm[47] because it runs four to six times faster for comparable precision. Initial values for the rate constants were estimated from experimental data or educated guesses. The rate constants were then varied by the modified simplex algorithm[48] to obtain a minimum in the error in the sum of the squares between calculated and experimental concentrations. The program is written in BASIC and was implemented on a Hewlett-Packard HP-86 computer. The program as implemented requires 10 min per iteration and typically 75 iterations to obtain convergence to one part in ten thousand in the error in the sum of the squares.

Results

Recently we reported[45] that irradiation of a rigorously degassed benzene or pyridine solution of $(FeTPP)_2O$ with an excess of PPh_3 results in spectral changes consistent with formation of $(py)_2FeTPP$ in pyridine, and $(PPh_3)FeTPP$ in benzene, and $OPPh_3$ in both. The rate of molar production of the Fe(II) complex is twice the rate of loss of $(FeTPP)_2O$ and twice the rate of gain of $OPPh_3$. We demonstrated that the quantum yield changes could best be fit by the following mechanisms:

$$(FeTPP)_2O \overset{h\nu}{\rightleftharpoons} (FeTPP)_2O^* \quad (1)$$

$$(FeTPP)_2O^* \xrightarrow{k_2} FeOTPP + FeTPP \quad (2)$$

$$FeTPP + FeOTPP \xrightarrow{k_3} (FeTPP)_2O \quad (3)$$

$$FeOTPP + PPh_3 \xrightarrow{k_4} FeTPP + OPPh_3 \quad (4)$$

$$FeTPP + B \xrightarrow{k_5} BFeTPP \quad (5)$$

$$BFeTPP + B \xrightarrow{k_6} B_2FeTPP \quad (6)$$

$$BFeTPP + FeOTPP \xrightarrow{k_7} (FeTPP)_2O + B \quad (7)$$

At low intensities, the k_3 pathway is negligible. In benzene, we assume $k_6 = 0$ and steady-state concentrations of $(FeTPP)_2O^*$, FeTPP, and FeOTPP to obtain eq 8. where ϕ_0 is the photodisproportionation quantum yield and ϕ_{obsd} is measured quantum yield for production of $(PPh_3)FeTPP$. In the case of pyridine (a much stronger base than PPh_3), k_6 is likely to be large, making the k_7 step negligible. Assuming additionally a steady-state concentration of BFeTPP leads to $\phi_{obsd} = 2\phi_0$, where ϕ_{obsd} is the measured quantum yield for production of $(py)_2FeTPP$. We obtained $\phi_0 = 1.0 \times 10^{-4}$, and $k_7/k_4 = 9.5 \times 10^4$.

$$\frac{1}{\phi_{obsd}} = \frac{1}{2\phi_0} + \frac{[BFeTPP]k_7}{4\phi_0 k_4[PPh_3]} \quad (8)$$

At high intensities and low concentrations of PPh_3 eq 8 breaks down. The failure of eq 8 is small but reproducible. It is found that at high intensities ϕ_0 is consistently lower than 1×10^{-4}, and the value of k_7/k_4 determined with this value of ϕ_0 is consistantly higher than that at lower intensities. These observations suggest that the steady-state assumption made on [FeTPP] is probably still valid; however, neglecting the k_3 path is not valid. Since inclusion of the k_3 path leads to an analytical solution in terms of the steady-state concentration of FeTPP, an unknown quantity, the high intensity data were computer fitted to the mechanism. In the computer model a steady-state concentration was assumed for $(FeTPP)_2O$ only, and the quantum yield at low intensities,

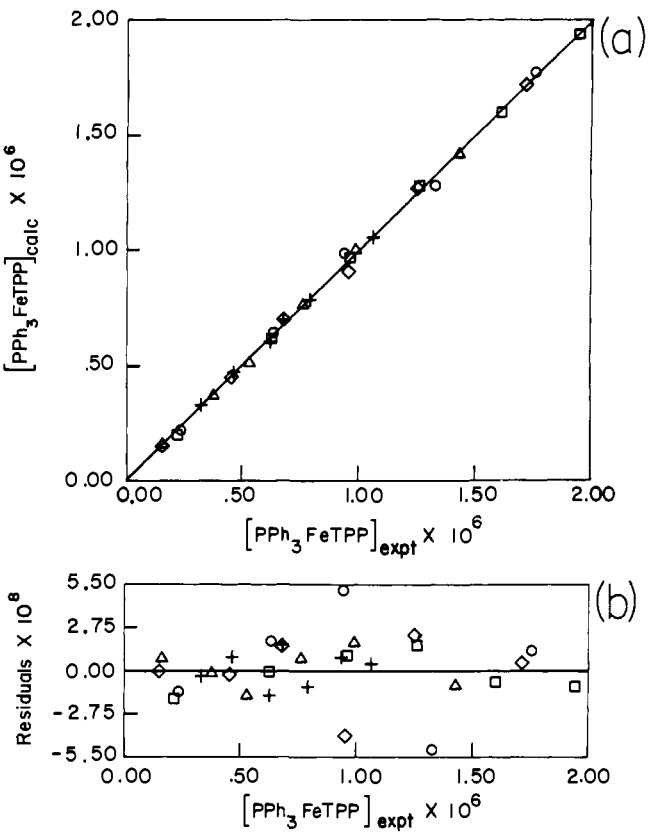

Figure 3. (a) Plot of experimental concentrations of $(PPh_3)FeTPP$ vs. those predicted from the kinetic model. Lamp intensities: ○, 3.10×10^{-8}; □, 2.95×10^{-8}; ◇, 2.16×10^{-8}; △, 8.8×10^{-10}; and +, 1.5×10^{-9} einstein. (b) Residuals.

1.0×10^{-4}, was assumed to be correct. The rate constants k_3, k_4, k_5, and k_7 were allowed to vary with *no restrictions*. Three experiments were simulated to find a common set of rates. These rates were then used to simulate other experiments at both high and low intensities.

Figure 3 shows the results of these fits for five different experiments and the residuals. It can be seen that the fit is quite good, yielding $k_3 = 1.26 \pm 0.01 \times 10^5\ M^{-1}\ s^{-1}$, $k_4 = 0.44 \pm 0.01$, $k_5 = 1.08 \pm 0.03$, and $k_7 = 4.23 \pm 0.10 \times 10^4$ (where the error reported represents the range of rates used to fit individual experiments). The ratio k_7/k_4 is found to be 9.6×10^4, in good agreement with the value of 9.5×10^4 reported earlier.

While the evidence is consistent with the photodisproportionation mechanism, it is difficult to conclusively disprove the existence of, say, $FeOTPP^-$ and $FeTPP^+$ among the primary photoproducts. Hence we sought direct spectroscopic observation of the primary photoproducts via laser flash photolysis.

Figure 4a depicts the transient absorption spectrum obtained 5 μs after excitation of a solution of $(FeTPP)_2O$ at 356 nm. The bleaching at ~408 nm is consistent with loss of $(FeTPP)_2O$, and the growths at ~434 and 525 nm are consistent with production of one oxo-coordinated FeTPP complex per dimer. This result at first seems surprising, since one would expect photoproduction of uncoordinated FeTPP; however, at μM levels of $(FeTPP)_2O$, it is quite possible that trace H_2O is coordinated to the $(FeTPP)_2O$ complex, and hence photodisproportionation leads directly to production of $H_2OFeTPP$. This rationale is supported by the work of Cohen.[49] He initially observed a magnetic susceptibility for $(FeTPP)_2O$ of 2.69 μ_B; however, after rigorously drying the sample, the moment was found to be 1.74 μ_B. The difference in the moments was attributed to H_2O coordinated in some fashion to the $(FeTPP)_2O$. Figure 4b is the difference spectrum obtained by computer simulating 1 mol of $(FeTPP)_2O$ minus 1 mol of $FeTPP(H_2O)$.[40] The agreement between the two spectra is good

(46) Gear, W. F. "Numerical Initial Value Problems in Ordinary Differential Equations"; Prentice-Hall: Englewood Cliffs, NJ, 1971.
(47) Rolston, A.; Wilf, H. "Mathematical Methods and Digital Computers"; Wiley: New York, 1960; p 110.
(48) Deming, S. N.; Morgan, S. L. *Anal. Chem.* **1973**, *45*, 278A.
(49) Cohen, I. A. *J. Am. Chem. Soc.* **1969**, *91*, 1980.

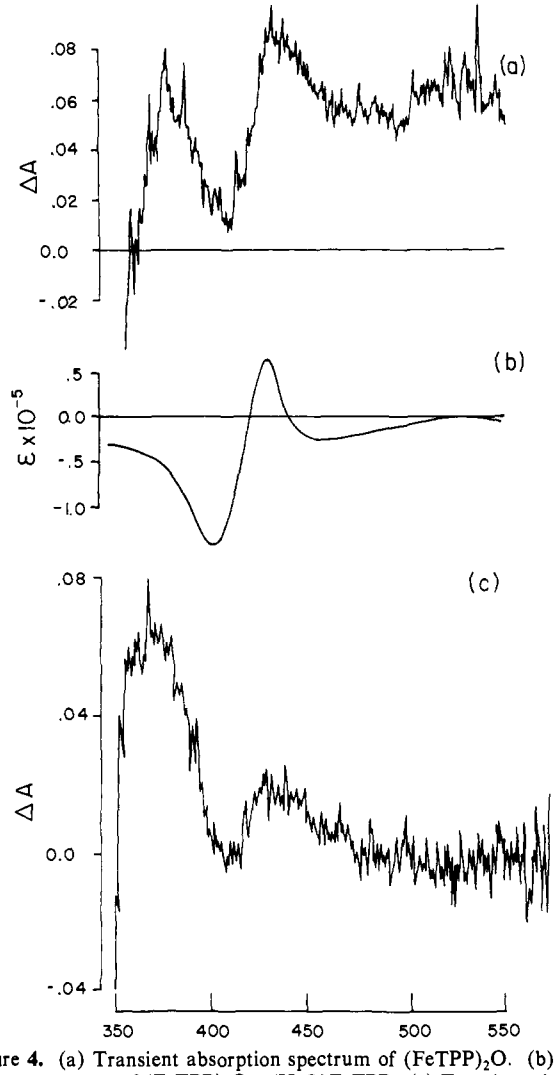

Figure 4. (a) Transient absorption spectrum of $(FeTPP)_2O$. (b) Difference spectrum of $(FeTPP)_2O - (H_2O)FeTPP$. (c) Transient absorption spectrum of $(FeTPP)_2O$ with care taken to resolve low wavelengths. Spectra recorded 5 μs after excitation at 355 nm in 1,2-dichloroethane.

in both peak positions (407 vs. 405, 434 vs. 432, and 525 vs. 525) and relative intensity.

The transient spectra obtained from 100 ns to 5.6 μs show no decay (within experimental error). This implies that cage recombination occurs rapidly while steady-state recombination is slow as predicted by the computer model; hence, neglecting the k_3 path in the mechanistic analysis is quite reasonable at low intensities.

Figure 4c shows the transient absorption spectrum of $(FeTPP)_2O$ with care taken to try to resolve the short wavelength region. This was done in an attempt to identify the ferryl complex, since the presence of a third signal is implied by the consistently positive OD in the long wavelength region (570–400 nm). It can be seen that a signal is growing in at ~370 nm. While the intensity seems at first rather large, it should be noted that this is a difference spectrum, and $(FeTPP)_2O$ has a relatively low extinction coefficient in this region. The observed transient is inconsistent with the ferryl porphyrin complex first observed by Balch and coworkers at 417–427 nm.[36] However, there was no base to coordinate the complex observed here. Even when pyridine was added (~50% v/v), no evidence was found for coordination to either FeTPP or the short wavelength transient (simply indicating that coordination of base to either complex is slow on this time scale). Noting that the general trend in the formation of Fe(III) porphyrin radical cations is to shift the Soret band to shorter wavelength (as much as 24 nm),[34] we postulate that in the absence of a good coordinating base, the ferryl complex exists as a Fe(III) radical cation rather than a Fe(IV) complex.

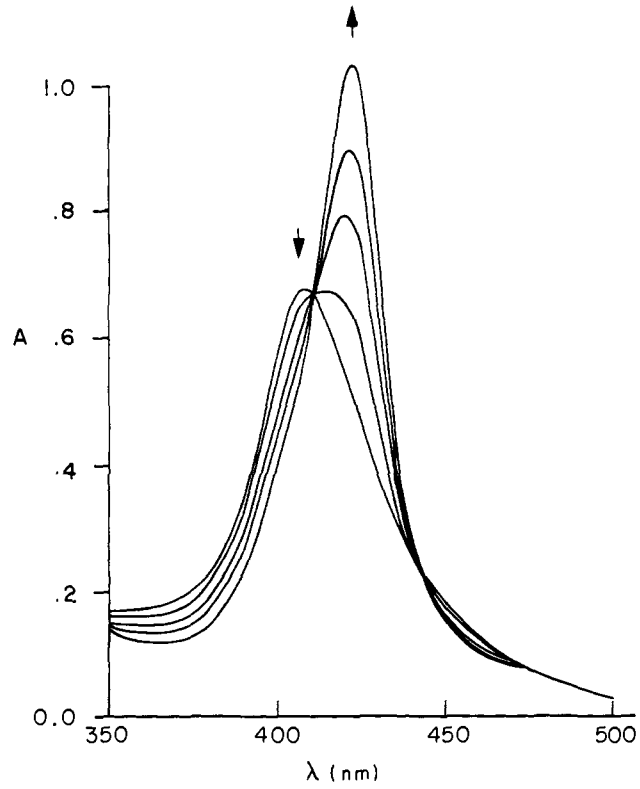

Figure 5. Photolysis of $(FeTPP)_2O$ in 5% cyclohexene/95% pyridine. Excitation at 409 nm; spectra taken at t = 0, 30, 50, 90, and 190 min of irradiation.

Similar results are obtained in the flash photolysis spectra of $(FeTPP)_2N$ and $(FeTPP)_2C$.[50] This also supports the radical cation assignment since the anticipated products from flash photolysis of $(FeTPP)_2N$ and $(FeTPP)_2C$ besides FeTPP for both would be "FeNTPP" and "FeCTPP", respectively. Both of the latter complexes may be formulated as Fe porphyrin radical cations (i.e., O–$Fe^{III}TPP^+$, N–$Fe^{IV}TPP^+$, and C–$Fe^{V}TPP^+$).

This evidence demonstrates that photodisproportionation is a new and useful technique for the photochemical generation of a strong oxidant, in this case, FeOTPP. However, the net reaction, air oxidation of PPh_3 to $OPPh_3$, is thermodynamically downhill, so it does not demonstrate net energy storage. In order to demonstrate the potential usefulness of this reaction, as well as to study the oxidative powers of the ferryl complex, other traps have been used.

Following Groves' (chloro)iron(III) porphyrin mediated oxidation of olefins,[28] cyclohexene and tetramethylethene (TME) were substituted for PPh_3. Unfortunately, no photochemistry is observed in either neat cyclohexene or TME after 3 h of irradiation at 409 nm ($I_0 = 1.5 \times 10^{-9}$ einstein). This is not surprising since the rate of trapping (k_4) would certainly be expected to be lower than that for PPh_3 and hence the slope of the Stern–Volmer plot much larger. Since results obtained in pyridine eliminated quenching of the photochemistry, mixed solvents of 5–95% pyridine 95–5% trap were used.

The photolysis of a 5% cyclohexene/95% pyridine solution of $(FeTPP)_2O$ is shown in Figure 5. As in the case of PPh_3, a clean reduction of $(FeTPP)_2O$ to FeTPP is observed. Similar results are obtained if cyclohexene is replaced with TME. The quantum yield for production of $(py)_2FeTPP$ in both cases is the same (at 409 nm) within experimental error as with PPh_3: $\phi = 2 \times 10^{-4}$. This implies that the ferryl complex is in some fashion oxidizing these olefins by two electrons.

To determine the nature of the organic photoproducts, the reaction was scaled up to millimolar levels with cyclohexene as

(50) Peterson, M. W.; Elliott, M. G.; Garrett, K. O.; Richman, R. M. *Inorg. Chem.*, submitted for publication.

the trap. Deoxygenation was performed by purging with argon and irradiations were carried out at a 450 W Hg lamp with Pyrex as a cutoff filter. TME could not be used for these purposes due to low solubility of $(FeTPP)_2O$ in the TME/pyridine mixed solvent. Both IR and NMR confirm cyclohex-2-en-1-ol as the major product (IR 3580, 1050, 955, 721 cm^{-1}; NMR δ 1.9 (7 H), 4.2 (0 H), and 5.81 (3 H)).

The nature of this oxidation is not readily apparent. The analogy of the radical mechanism proposed by Groves for cytochrome P-450 seems reasonable. However, in the scaled up work products other than cyclohex-2-en-1-ol were present, perhaps due to other radical processes. To test for the presence of radicals during photolysis, the ESR spin trap PBN was added to a pyridine/cyclohexene and a pyridine/TME solution of $(FeTPP)_2O$ and irradiated in an ESR cavity. It should be noted that only this combination results in a signal. Removing any one of the compounds causes no signal to be produced at reasonable irradiation times. In both cases, a typical nitrone adduct is formed at relatively short irradiation times ($\sim$0.5 h) with a_N = 14.8 G and a_H = 2.4 G for cyclohexene, and a_N = 14.6 G and a_H = 2.33 G for TME. The two radicals have different hyperfine coupling constants, neither of which may be attributed to pyridine radical or PBN decomposition products.[50,52] This supports a radical mechanism where the radicals formed need not react solely with the ferric complex. That is

$$(FeTPP)_2O \overset{h\nu}{\rightleftharpoons} Fe^{IV}OTPP + Fe^{II}TPP$$

$$Fe^{IV}OTPP + \text{allyic hydrogen atom} \rightarrow Fe^{III}OHTPP + \text{olefin}\cdot$$

$$Fe^{III}OHTPP + \text{olefin}\cdot \rightarrow Fe^{II}TPP + \text{olefin–OH}$$

$$\text{olefin}\cdot + \text{substrate} \rightarrow \text{olefin} + \text{substrate}\cdot$$

The main difference from the P-450 mechanism is the ability of the olefin radical to escape the initially formed cage complex. This result is also supported by photolysis in the presence of O_2, as outlined below.

Having demonstrated that FeOTPP may be used to oxidize olefins, we wanted to determine if a catalytic process could be established.

The mechanism by which FeTPP reacts with O_2 to form $(FeTPP)_2O$, as outlined by Balch and co-workers,[36] is

$$2Fe^{II}TPP + O_2 \rightarrow (Fe^{III}TPP)_2O_2$$

$$(Fe^{III}TPP)_2O_2 \rightarrow 2Fe^{IV}OTPP$$

$$Fe^{IV}OTPP + (Fe^{III}TPP)_2O_2 \rightarrow (Fe^{III}TPP)_2O + O_2Fe^{II}TPP$$

$$O_2Fe^{II}TPP + Fe^{IV}OTPP \rightarrow (Fe^{III}TPP)_2O + O_2$$

Hence, O_2 might not only act as a trap for FeTPP but in the process also produce the ferryl complex.

To test the ability of O_2 to trap the ferrous complex during photolysis, a benzene solution of $(FeTPP)_2O$ was irradiated in the presence of 1 atm of O_2. It is observed that there is a net bleaching of the initial spectrum. This result can only be explained by a radical reaction which attacks the porphyrin ring. Since in the absence of O_2 no photochemistry is observed, it can be assumed that the O_2 is in fact trapping the ferrous complex, resulting in a net buildup of the ferryl complex, which in turn initiates some type of destructive radical reaction.

On the basis of the ability of O_2 to trap the ferrous complex, O_2 might serve the function of pyridine (i.e., prevent ferryl–ferrous recombination) in the case of oxidation of olefins, and it should then lead to a catalytic oxidation. To test this, two experiments were performed. The first was irradiation of a cyclohexene solution of $(FeTPP)_2O$ ($\sim 5 \times 10^{-3}$ M) with sunlight over a period of 3 months. The second was irradiation of a similar solution at a 450 W Hg lamp for a period of 37 h. From these two experiments, two results are obtained.

Table I. Quantum Yield Data for $(FeTPP)_2O$

λ_{excite}	T, K	$[PPh_3]$	solvent	$(\phi_0 \times 10^5) \pm 10\%$
441	296.5	0.1	py/benzene	4
437	296.5	0.1	benzene	4
409	296.5	0.05	py/benzene	10
	296.5	0.1	benzene	10
	283	0.1		9.7
	293	0.1		10
	303	0.1		9.8
380	296.5	0.05	py/benzene	29
	283		benzene	28
	293			29
	303			28
365	296.5	0.05	py/benzene	69
	296.5		benzene	76
	283			75
	293			76
	303			76
350	296.5	0.005	py/benzene	163

At the low intensities represented by available sunlight, the sole organic product obtained was cyclohex-2-en-1-one as determined by IR and NMR (IR 1680, 1382, 935, and 725 cm^{-1}; NMR δ 2.4 (6 H), 6.0 (2 H), and 7.1 (2 H)). $(FeTPP)_2O$ showed no detectable degradation and converted $\sim$20% of the cyclohexene to cyclohex-2-en-1-one (determined by NMR; it should be noted that here a radical chain reaction occurs). At high intensities, on the other hand, the primary product is cyclohex-2-en-1-ol (with detectable amounts of cyclohex-2-en-1-one). Again, there was no detectable loss of $(FeTPP)_2O$ and in this case, there were $\sim$1000 turnovers of $(FeTPP)_2O$ (based on $(FeTPP)_2O \rightarrow$ 2FeOTPP).

These results imply a strong intensity dependence in the nature of the radical reaction and may be rationalized on the basis of the following mechanism

$$(FeTPP)_2O \overset{h\nu}{\rightleftharpoons} (FeTPP)_2O^* \quad (1)$$

$$(FeTPP)_2O^* \rightarrow FeTPP + FeOTPP \quad (2)$$

$$\text{olefin} + FeOTPP \rightarrow FeOHTPP + \text{olefin}\cdot \quad (9)$$

$$\text{olefin}\cdot + FeOHTPP \rightarrow FeTPP + \text{HO—olefin} \quad (10)$$

$$2\text{olefin}\cdot \rightarrow \text{olefin—olefin} \quad (11)$$

$$2FeOHTPP \rightarrow (FeTPP)_2O + H_2O \quad (12)$$

$$O_2 + \text{olefin}\cdot \rightarrow\!\!\rightarrow \text{O=olefin} \quad (13)$$

An analysis of this mechanism (excluding step 13) leads to the following conditions for successful production of cyclohex-2-en-1-ol in the absence of O_2: $k_{10} > (k_{11}k_{12})^{1/2}$ At low intensities, step 10 (which will go as I_0^2) will be less important than step 13 (i.e., $k_{13} > k_{10}$), leading to ketone formation. At high intensities, step 10 becomes dominant, leading to alcohol production.

These results also account for the observation of Paulson and co-workers.[53] They reported that $(FeTPP)_2O$ would catalyze the O_2 oxidation of olefins. We were unable to reproduce these results after allowing a cyclohexene solution of $(FeTPP)_2O$ to sit in the dark for 3 months and, in fact, observed no reaction whatsoever. The procedure used by Paulson to generate $(FeTPP)_2O$ was the O_2 oxidation of FeTPP in the presence of the olefin to be oxidized. This is known to produce FeOTPP as an intermediate, which can then follow eq 9–13.

Initially, we speculated that the photoactive transition in $(FeTPP)_2O$ was lmct or mlct.[45] To determine the nature and location of the photoactive excited state, the wavelength dependence and the temperature dependence of the quantum yield were studied. These results are summarized in Table I.

Figure 6 shows the short wavelength spectrum of $(FeTPP)_2O$. The transition at 316 nm is intriguing since it is not observed in

(51) Janzen, E. G. *Acc. Chem. Res.* **1971**, *4*, 31.
(52) Janzen, E. G.; Blackburn, H. J. *J. Am. Chem. Soc.* **1969**, *91*, 4481.
(53) Paulson, D. R.; Ullman, R.; Sloane, R. B.; Closs, G. L. *J. Chem. Soc., Chem. Commun.* **1974**, 186.

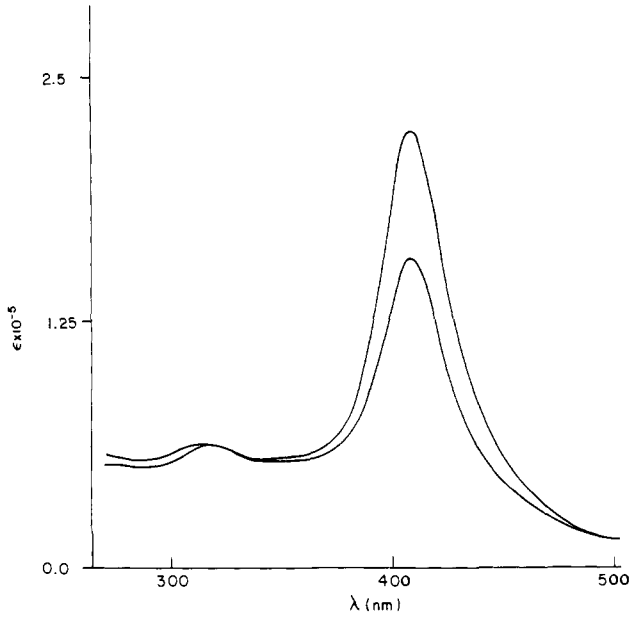

Figure 6. Spectra of $(FeTPP)_2O$ in 1,2-dichloroethane (higher absorbance at 400 nm) and $(FeTPPC)_2O$ in pH 10 buffer.

the isostructural dimers, $(FeTPP)_2N$ and $(FeTPP)_2C$. Unfortunately, the quantum yields can only be determined down to ~350 nm. This is due to the necessity of using benzene/PPh_3. Attempts were made to use cyclohexene/piperidine; however, the quantum yields were irreproducible (presumably due to radical reactions that complicate the system) and lower than with PPh_3. The data to 350 nm do demonstrate a strong dependence on wavelength, implying that perhaps the state at 316 nm is the photoactive one. However, the nature of this transition remains speculative.

The low value of the quantum yield at long wavelength should allow for estimation of the apparent activation energy[4,54] by following the temperature dependence since

$$\phi_0 = \frac{k_2}{k_2 + k_{-1}} = \frac{k_2}{k_{-1}}$$

Hence, if k_{-1} is assumed to be temperature independent

$$\phi_0 \simeq A \exp(-E_a/RT)/k_{-1}$$

or

$$\ln(\phi_0) = \ln(A/k_{-1}) - E_a/RT$$

Much to our surprise, the quantum yield shows no temperature dependence (Table I).

These results, while not definitive, do seem to indicate that perhaps a photomechanism other than lmct or mlct is active. However, a larger body of evidence is needed to firmly establish the nature of the photomechanism. This will be addressed further, in light of our recent results on the analogous complex $(FeTPPC)_2O$) (TPPC = tetra(4-carboxyl)phenylporphyrin)).[55]

Discussion

The experimental observations for both complexes $(FeTPP)_2O$ and $(FeTPPC)_2O$[55] may be summarized as follows. (1) Neither complex is photoactive at wavelengths longer than 500 nm ($\phi_0 < 1 \times 10^{-6}$). (2) Both complexes show a quantum yield increasing with decreasing wavelength (Figure 7). (3) Neither complex shows detectable emission below 800 nm ($\phi_0 < 1 \times 10^{-4}$). (4) Flash photolysis shows no detectable heterolytic cleavage of the Fe–O bond (to form $FeTPP^+$ and $FeTPP\text{–}O^-$). (5) $(FeTPP)_2O$ shows no temperature dependence in its quantum yield at wavelengths up to 409 nm (Table I). (6) Both complexes have a transition around 320 nm that has not been assigned (Figure 6). (7) The quantum yield for $(FeTPPC)_2O$ flattens out short

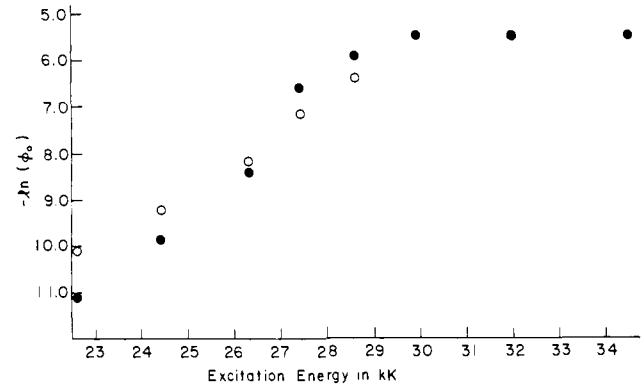

Figure 7. Plot of ln (ϕ_0) vs. excitation energy for (O) $(FeTPP)_2O$ and (●) $(FeTPPC)_2O$.

wavelengths (Figure 7). Each of these observations must be considered in formulating an appropriate photomechanism.

Three photomechanisms will be considered to explain the wavelength dependence of the quantum yield. They are that these complexes are reacting (1) from a hot ground state,[54] (2) in the strong coupling limit,[56,57] and (3) from a highly distorted charge-transfer state.[58,59]

In the hot ground-state mechanism, it is assumed that internal conversion produces a ground state with an excess of thermal energy. This molecule then dissociates with some probability within the interval of cooling off by vibronic relaxation. This probability, and hence the quantum yield, should increase with decreasing wavelength since the molecule has available more energy and a longer time interval for dissociation.

This photomechanism may be eliminated on the basis of three observations. The first observation is that there is no temperature dependence in the quantum yield at long wavelengths even though this photomechanism would be expected to produce such a dependence at wavelengths close to the threshold energy for dissociation.[54] The second observation is that these complexes have a large number of normal modes of vibration available for cooling off and hence the threshold energy for dissociation would be expected to be unrealistically low. This is evident from Zimmerman's equation[54] that describes the anticipated wavelength dependence of the quantum yield

$$\phi = \left(1.0 - \frac{E_0}{E}\right)^N \qquad (14)$$

where E is the excitation energy, E_0 is the threshold energy (e.g., the energy of the Fe–O bond), and N is the number of normal modes of vibration for cooling. E estimated from this equation with 477 normal modes is less than 0.5 kcal. The final inconsistent observation is that the quantum yield for dissociation stops increasing at sufficiently short wavelengths for $(FeTPPC)_2O$. While one might envision a second competing type of photochemistry that accounts for this (e.g., exchange of axially coordinated H_2O or perhaps heterolytic bond cleavage), this seems unlikely. Its wavelength dependent quantum yield would have to parallel that of the photodisproportionation, and the flash photolysis of these complexes shows no transients consistent with either alternative type of photochemistry.[55]

The second potential photomechanism is that these molecules are reacting in the strong coupling limit.[56,57] Under these conditions, the nature of the electronic transition is less important than the vibronic state and its ability to couple to the dissociation continuum. The difference between the hot ground state and

(54) Zimmerman, G. *J. Chem. Phys.* **1955**, *23*, 825.
(55) Peterson, M. W.; Richman, R. M. *Inorg. Chem.* **1985**, *24*, 722.
(56) Johnson, C. E.; Trogler, W. C. *J. Am. Chem. Soc.* **1981**, *103*, 6352.
(57) Jortner, J.; Rice, S. A.; Hochstrasser, R. M. *Adv. Photochem.* **1969**, *7*, 149.
(58) Porter, G. B.; Doering, J. G.; Karanku, S. *J. Am. Chem. Soc.* **1962**, *84*, 4027.
(59) Balzani, V.; Ballardini, R.; Sabbatini, N.; Moggi, L. *Inorg. Chem.* **1968**, *7*, 1398.

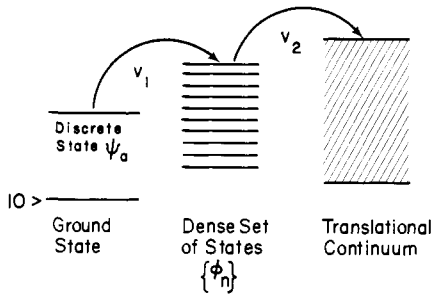

Figure 8. Energy level scheme for the zero-order states and coupling necessary for photodissociation.

strong coupling limit mechanisms is subtle and merits a brief discussion.

In the hot ground state the dissociation occurs from a particular vibrational mode (e.g., the antisymmetric stretch of M–O–M). Anharmonic coupling between normal modes leads to internal energy transfer until a sufficient amount of energy is collected in the particular mode to cause dissociation. Since a larger number of vibrational modes will lead to more efficient dissipation of the excess thermal energy, the efficiency of the photochemistry will drop off (see eq 14). The strong coupling limit, on the other hand, requires an extremely large number of vibrational modes (i.e., the "statistical limit).[57] In this mechanism, our concern is the way in which the zero-order excited-state wave function (a discrete level) will couple to a dense set of vibrational levels belonging to a different electronic state (due to the large number of modes) that couples to the translational continuum (see Figure 8).[57]

This leads to predissociation from a band of states and not from a single state. In this case, no specific mode of vibration is responsible for dissociation. Therefore, excited-state energy is converted into vibrational motion within the molecule which then may lead to dissociation before vibrational deactivation. No specific correlation can be inferred between the number of vibrational modes and the quantum yield since the rates for both internal conversion and dissociation depend on the nature of the excited-state coupling (both electronic and vibronic coupling). However, such a process will have a lifetime of a form similar to that derivable from Fermi's golden rule.[57]

The experimental manifestations of this photomechanism outlined by Trogler and Johnson[56] are the following: (1) quantum yields for photodissociation depend on the amount by which the excitation energy exceeds the thermodynamic threshold; (2) multiple reaction pathways become increasingly available at higher excitation energies; (3) there should be a structure sensitivity to the quantum yields; and (4) the exact antibonding nature of the excited state becomes irrelevant. A further manifestation is that there should be no thermal or solvent dependence in the quantum yield.

The dimers studied to data fit this model well. $(FeTPP)_2X$ dimers (X = O, N, and C) all show an exponential dependence of their quantum yields on excitation energy, with $(FeTPP)_2N$ studied down to 313 nm and $(FeTPP)_2C$ to 260 nm.[50] The only exception to this wavelength dependence is $(FeTPPC)_2O$; however, the flattening of the quantum yield might be due to photodissociation of coordinated H_2O (i.e., point 2 above) at short wavelengths. A closer look, however, shows several inconsistencies. First, $(FeTPP)_2C$ also has coordinated H_2O, yet this has no effect on the quantum yield at short wavelength. The threshold energy for photodissociation of H_2O would be expected to be much less than that of the Fe–O or Fe–C bond (in fact, $(FeTPPC)_2O$ thermally exchanges H_2O on an NMR time scale). The threshold energy (and hence the reciprocal of the quantum yield) would be expected to increase in the order Fe–O, Fe–N, and Fe–C, on the basis of the ability of the bridging atom to form π bonds to the metal centers. This is not the case. While $(FeTPP)_2N$ is found be have a lower quantum yield than $(FeTPP)_2O$ (and hence a lower observed threshold energy), $(FeTPP)_2C$ is found to have a higher quantum yield and lower observed threshold energy. Photochemistry is observed up to 530 nm with $(FeTPP)_2C$; however, the lower threshold energy may be due to weaker σ bonding in the Fe–C bond than in either $(FeTPP)_2O$ or $(FeTPP)_2N$.

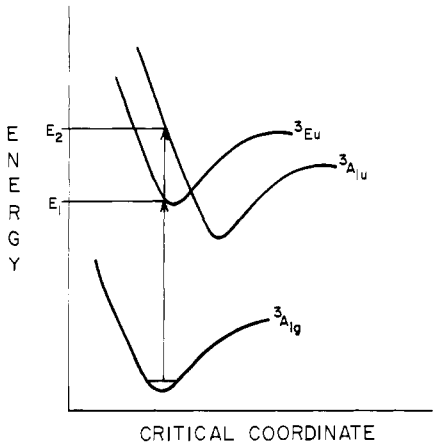

Figure 9. Schematic representation of a highly distorted charge transfer and Soret excited states for $(FeTPP)_2O$ or $(FeTPPC)_2O$. E_1 and E_2 represent the transition energy. The critical coordinate will, in general, be different from that depicted in Figure 2.

The existence of a highly distorted charge-transfer state seems likely, considering the nature of such a state. Figure 2 depicts a potential energy surface that might lead to disproportionation. A vertical transition leads to a highly distorted excited state. If this excited state leads to dissociation, the success of the photo event in leading to the fragments M and M=O could be wavelength dependent in that the probability of escaping the initial solvent cage would depend on the amount of vibronic energy that is translated into translational energy in the fragments and hence the vibronic state from which it dissociates.[1]

The proposed excited state differs from conventional (though it does have precedence[58,59]) CT photochemistry in two ways. (1) The CT excited state is highly distorted presumably due to a change in bond order of the bridging M–O–M system; and (2) photoreaction occurs directly from the excited vibronic state (i.e., not from a thexi state).[4] This might be thought of as a cross between the SCL and CT photomechanisms, that is, both the antibonding nature of the excited state and the vibronic state excited determine the efficiency of the observed photochemistry. This represents intermediate coupling within the excited-state manifold.[55]

Such a situation is depicted in Figure 9 where the first excited state represents the ligand localized $\pi \rightarrow \pi^*$ state (E_u) and the second excited state (A_{1u}) represents the photoactive state. Since we observe the vertical (Franck–Condon) transition in UV–vis spectroscopy, it would appear that the A_{1u} state is higher in energy than the Soret state, but this is clearly not the case. Internal conversion would lead to population of the photoactive state and hence the appearance that the Soret band is photoactive. (Here we have not been specific about the nature of the "critical coordinate" since distortion of the excited state would probably involve movement of the iron atoms relative to the porphyrin ring plane as well as the oxygen bridge.) This explanation may well have general utility in the understanding of the photochemistry of many nonemitting metalloporphyrin complexes.

The notion of a highly distorted excited state is supported by the observation that only $(FeTPP)_2O$ and $(FeTPPC)_2O$ have a well-defined transition at ~320 nm (Figure 6) and that in $(FeTPPC)_2O$ the quantum yield begins to flatten out in this region. If the 320-nm transition is a measure of the photoactive transition energy (i.e., the zero-point energy difference) then it might well be at even higher energy in $(FeTPP)_2N$ and $(FeTPP)_2C$, since the observed Franck–Condon transition energy will depend on the extent of excited-state distortion. (No well-defined transition is observed in $(FeTPP)_2C$; however, $(FeTPP)_2N$ does have a transition at ~280 nm that might be associated with the one at 320 nm in the oxo-bridged complexes.)

The key to observing photodisproportionation in the iron porphyrin dimers may well rest in their simple and rigid structures.

Thus both ligand exchange and radical formation are not observed, leaving photodisproportionation as the only process leading to observable photochemistry.

Figure 10 shows an extended Hückel calculation of the valence orbitals for the $N_4Fe–O–FeN_4$ fragment.[60] The lowest triplet-to-triplet transition from this diagram involves the Fe–O–Fe core and is the $e_u \leftarrow e_g$. This leads to four excited states: $^3A_{1u}$, $^3A_{2u}$, $^3B_{1u}$, and $^3B_{2u}$. These states may be formulated as:

$$^3B_{2u} \quad e_g^x(1)e_u^x(2) + e_g^x(2)e_u^x(1) - e_g^y(1)e_u^y(2) - e_g^y(2)e_u^y(1)$$

$$^3A_{2u} \quad e_g^x(1)e_u^x(2) + e_g^x(2)e_u^x(1) + e_g^y(1)e_u^y(2) + e_g^y(2)e_u^y(1)$$
$$\}(\alpha(1)\beta(2) - \alpha(2)\beta(1))$$

$$^3A_{1u} \quad e_g^x(1)e_u^y(2) + e_g^x(2)e_u^y(1) + e_g^y(1)e_u^x(2) + e_g^y(2e)_u^x(1)$$

$$^3B_{1u} \quad e_g^x(1)e_u^y(2) + e_g^x(2)e_u^y(1) - e_g^y(1)e_u^x(2) - e_g^y(2)e_u^x(1)$$

Expanding in terms of the d orbitals (O p orbital contribution is again taken to be small):

$$\psi_{A_{2u}} = (d^1_{xz}(1)d^1_{xz}(2) + d^1_{yz}(1)d^1_{yz}(2) - d^2_{xz}(1)d^2_{xz}(2) - d^2_{yz}(1)d^2_{yz}(2))$$

$$\psi_{B_{2u}} = (d^1_{xz}(1)d^1_{xz}(2) - d^1_{yz}(1)d^1_{yz}(2) + d^2_{xz}(1)d^2_{xz}(2) - d^2_{yz}(1)d^2_{yz}(2))$$

$$\psi_{A_{1u}} = (d^1_{xz}(1)d^1_{yz}(2) + d^1_{yz}(1)d^1_{xz}(2) - d^2_{xz}(1)d^2_{yz}(2) - d^2_{yz}(1)d^2_{xz}(2))$$

$$\psi_{B_{1u}} = (d^2_{xz}(1)d^1_{yz}(2) + d^1_{xz}(1)d^2_{yz}(2) - d^1_{xz}(2)d^2_{yz}(1) + d^2_{xz}(2)d^1_{yz}(1))$$

The $^3A_{2u}$, $^3A_{1u}$, and $^3B_{2u}$ excited states may be formulated in a valence bond description as

$$M^+OM^- \pm M^-OM^+$$

which we interpret as metal-to-metal charge transfer. The $^3B_{1u}$ excited state represents a state that might be interpreted as a metal-localized d–d excited state that might tend toward axial ligand exchange rather then disproportionation.

It is emphasized that this treatment of the excited-state manifold is vastly oversimplified. The electronic structure and spectra of porphyrins and metalloporphyrins have been the subject of extensive theoretical study.[9,10] Some transitions in the complex visible spectra of metalloporphyrins are generally attributed to configuration interaction between metal-centered d orbitals and the porphyrin orbitals. In the above treatment only the limited metal–oxygen orbital interactions have been considered with no consideration of porphyrin orbitals. Hence, one might be tempted to interpret the wavelength dependence of the quantum yield as due to excited-state mixing of the MOM transition and the porphyrin $\pi \rightarrow \pi^*$ transition, thus leading to photoactivity in the Soret region. This may have some effect; however, it can be largely disregarded for two reasons. First, the quantum yield is monotonically increasing through the Soret region. This would not be expected. Rather the quantum yield should flatten within each transition at a value that reflects the extent of mixing and the absolute quantum yield for the photoactive excited state. Secondly, the excited states that would be required to mix are of the wrong symmetry: $\pi \rightarrow \pi^*$ is of E_u symmetry.

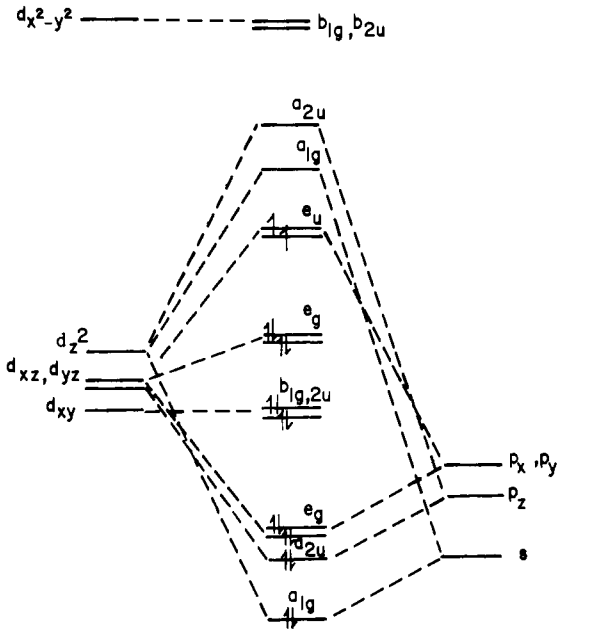

Figure 10. Molecular orbital diagram for $N_4Fe^{III}–O–Fe^{III}N_4$. (Orbital ordering taken from ref 60. D_{4h} symmetry labels are used here.

Conclusion

Photodisproportionation has been demonstrated in aprotic solvents for a μ-oxo-bridged iron porphyrin complex. Both continuous and flash photolysis confirm disproportionation directly from the excited state. A strong one-electron oxidant, the ferryl complex, is produced. Catalytic oxidation of olefins can be performed by photolyzing $(FeTPP)_2O$ in the presence of both dioxygen and olefin. All photochemical/physical observations including the quantum yield/wavelength profile are consistent with photochemistry occurring from a highly distorted charge-transfer excited state that may be viewed as an intervalence charge-transfer state. While the quantum yield is small throughout the wavelength region studied, appropriate modification of this system may lead to a useful technique for solar energy conversion.

Acknowledgment. This work was supported by the Office of Basic Energy Sciences of the Department of Energy.

(60) Tatsumi, K.; Hoffmann, R. *J. Am. Chem. Soc.* **1981**, *103*, 3328.